

Chemical Diagnostics for Tracing the Physical Structures in Disk-Forming Regions of Young Low-Mass Protostellar Sources

Yoko Oya

Yukawa Institute for Theoretical Physics, Kyoto University

Abstract. To understand the chemical origin of the Solar system, the chemical evolution along the star/planet formation is a key issue. Extensive observational studies have demonstrated a chemical diversity in young low-mass protostellar sources so far. Furthermore, chemical differentiations in the vicinity of the protostars have recently been reported. This suggests that molecular distribution is sensitive to a change in the physical conditions associated with disk formation. Some kinds of molecular lines, especially Sulfur-bearing species, are therefore prospected to work as molecular markers to highlight particular structures of disk-forming regions.

Conversely, detailed physical characterization is essential for elucidating the chemical evolution occurring there. Machine learnings may help us to disentangle the observed structures. Angular momentum of the gas is the key topic to understand the structure formation, which is also essential to the integration of the chemical and physical characterization.

Keywords. astrochemistry, stars: protostars, stars: low-mass, stars: kinematics and dynamics, protoplanetary discs

1. Introduction

To explore the chemical origin of the Solar system, the chemical evolution along the star/planet formation has been extensively examined. For instance, the chemical compositions in its earlier phase (protostellar cores) have been observed at the radio wave-length. That in the later phase (planetary systems) has been examined by sample return missions within the Solar system. The intermediate phase is that for the formation of protostellar/protoplanetary disks, where a surprisingly wide variety of organic molecules are produced. While theoretical studies have been performed extensively for this phase, the observational studies had a longstanding missing link. Atacama Large Millimeter/submillimeter Array (ALMA) has given large impacts on this field in this decade.

In spite of these efforts, it is still observationally controversial ‘*when and how disks are formed around a newly-born protostar*’ and ‘*what kinds of molecules are delivered into disks*’. These important issues in astrophysics and astrochemistry are also related with the diversity in planetary systems.

2. Organic Molecules in Disk-Forming Regions

It is known that low-mass protostellar cores show a chemical diversity (e.g. [Lefloch et al. 2018](#)). For instance, two distinct cases are the hot corino chemistry and warm carbon-chain chemistry (WCCC). Hot corinos are rich in complex organic molecules (COMs; e.g. CH₃OH, CH₃CHO) (e.g. [Schöier et al. 2002](#); [Ceccarelli 2004](#)). WCCC sources are rich in unsaturated hydrocarbons (e.g. CCH, c-C₃H₂) (e.g. [Sakai & Yamamoto 2013](#)). *How these diversities are evolved toward planetary systems* is an important clue to the material origins of the Solar system.

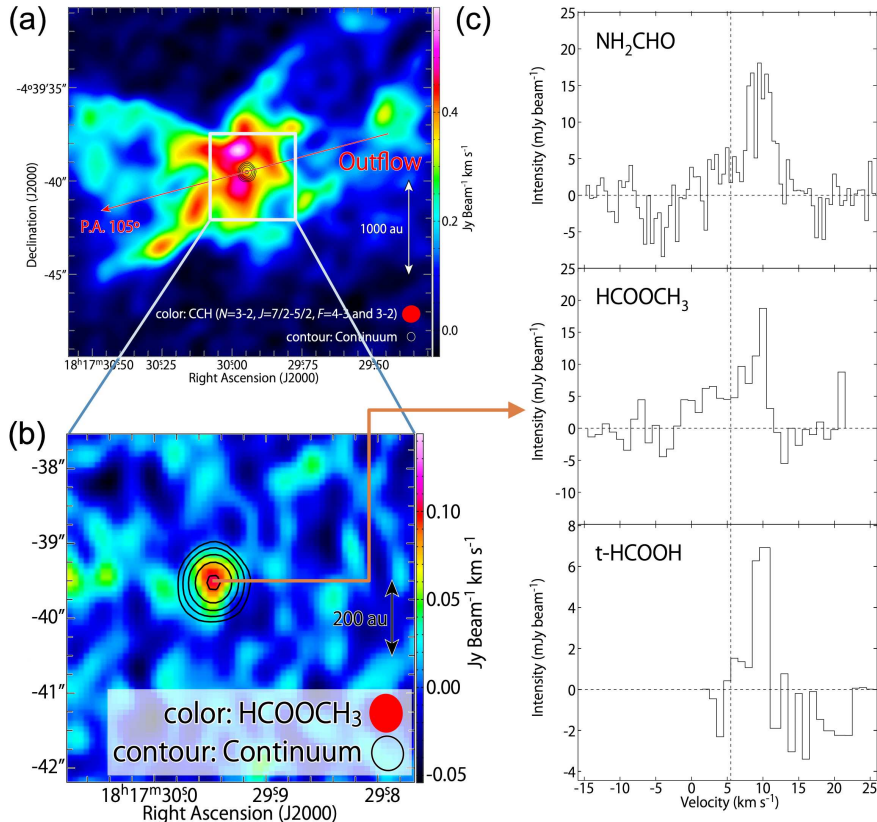


Figure 1. (a, b) Integrated intensity maps of the CCH emission (a; color) and the HCOOCH₃ emission (b; color) toward L483 observed with ALMA. Contours represent the 1.2 mm continuum emission. Distributions of the emission of hydrocarbons are spread over 10^3 au, while those of COMs are concentrated to the protostellar position. (c) Spectra toward the protostellar position showing the detection of COMs. Panels are taken from Oya et al. (2017) with modifications.

2.1. Chemical Differentiation within One Source

The chemical diversity in protostellar cores was recently found to be interpreted as a single picture in disk-forming regions (Oya 2022). The above two distinct cases have been thought to be exclusive to each other; however, some protostellar sources were found to show both of these chemical characteristics.

L483 is an example with such a ‘hybrid’ chemical characteristics (Figure 1). L483 is a dark cloud core located in Aquila Rift ($d = 200$ pc; Rice et al. 2006), which harbors a Class 0 low-mass protostellar source IRAS 18148–0440 (Fuller et al. 1995). ALMA observations revealed that the emissions of hydrocarbons are detected in the extended envelope gas and the outflow lobes in this source (Oya et al. 2017, 2018). Meanwhile, the emissions of COMs were detected only in the vicinity of the protostar. It is interesting that the two different chemical characteristics are spatially separated.

The chemical differentiation of organic molecules found in L483 has been confirmed in other sources with the hybrid chemical characteristics (B335, CB68; Imai et al. 2019, 2022). These observational results are actually consistent with a chemical model for a dynamically collapsing core reported by Aikawa et al. (2008). Figure 2 shows the radial profiles of the

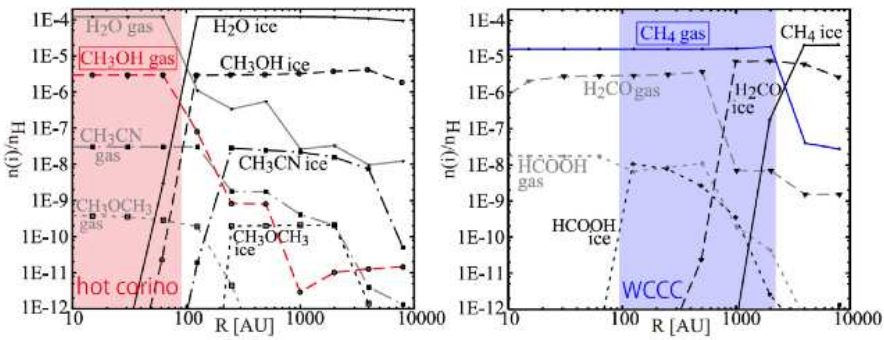


Figure 2. Plots of the molecular abundances as a function of the distance to the protostar. Plots are taken from Aikawa et al. (2008) with modifications.

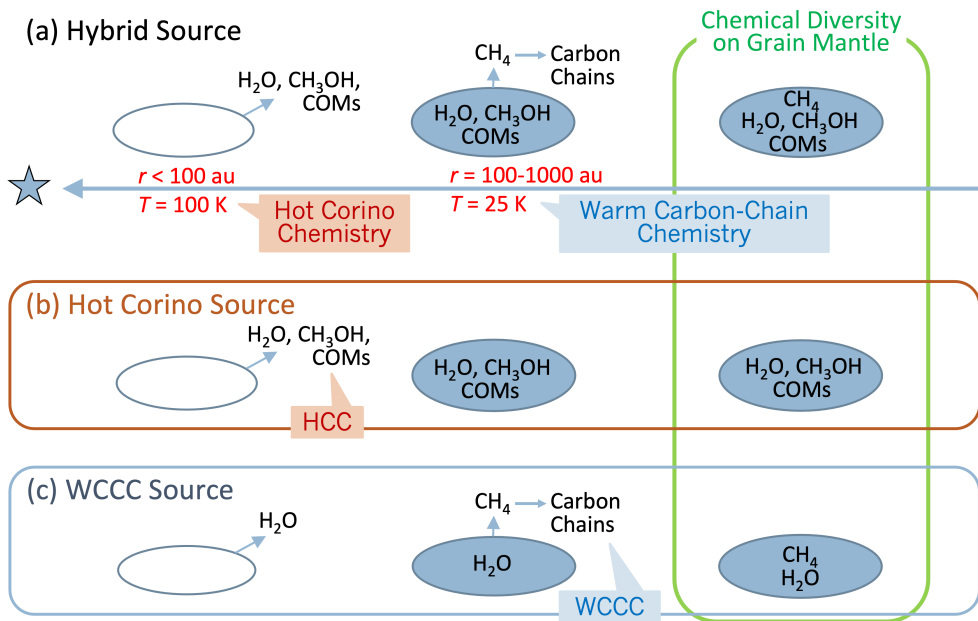


Figure 3. Schematic illustration of the sublimation of molecules from dust grains.

molecular abundances in the chemical model. CH_3OH is seen in the gas-phase at a distance $< 10^2$ au from the protostar; it is sublimated from dust grains in the hot regions near the protostar, as known as the hot corino activity. Meanwhile, CH_4 is seen in the gas-phase in the warm region with a distance from 10^2 au to 10^3 au from the protostar. The difference in these molecular distributions in the gas-phase can be attributed to the difference in their desorption temperatures; CH_3OH and other COMs are thought to be sublimated from the dust grains with water at a dust temperature > 100 K, while CH_4 at a dust temperature > 25 K.

Figure 3 shows a simplified view for the sublimation of organic molecules from dust grains. The case for sources with the hybrid chemical characteristics is shown in Figure 3(a). First, various molecular species exist in grain mantles, as shown at the right end in this panel. Grains fall into a warm region ($T > 25$ K), leading the sublimation of CH_4 . Enhancement of CH_4 in

the gas-phase triggers efficient production of hydrocarbons (i.e. WCCC). Then, grains fall into a hot region ($T > 100$ K), and water and COMs are sublimated (i.e. hot corino activity). This can be regarded as the basic picture.

2.2. Chemical Variety among Sources

The situation described above depends on the initial chemical condition of dust grains. Figure 3(b) shows a case where CH_4 is deficient in dust grains. The abundance of CH_4 in the gas-phase is depressed in a warm region, while COMs are sublimated in a hot region; this case corresponds to hot corino sources. Alternatively, a case deficient in COMs is shown in Figure 3(c). Hydrocarbons can be produced from CH_4 sublimated in a warm region, while the enhancement of abundance of COMs is not expected to be significant in a hot region; this case is regarded as WCCC sources. In summary, the chemical diversity in protostellar sources are likely originated from that on a grain mantle, which is expected to be determined according to the physical and chemical conditions in the prestellar stage.

The chemical composition of a grain mantle mainly depends on what kinds of molecules deplete on a grain and how they are accumulated on a grain during the cold starless phase. More specifically, it is proposed to depend on the duration time of the starless-core phase. If the duration time is long enough, a significant rate of carbon atoms are converted to CO molecules in the gas phase before their adsorption, and produced CO molecules are accumulated on dust grains. Then, CO can form a variety of COMs via dust surface reactions, which will show the hot corino chemistry in the vicinity of a protostar. On the contrary, carbon atoms are depleted onto dust grains as they are, if the duration time is too short to convert them to CO molecules. Then, carbon atoms will be hydrogenated to CH_4 on dust surface, which will trigger WCCC. The duration time can be moderate; both of carbon atoms and CO molecules will exist on dust grains, resulting in the hybrid chemistry (Figure 3a). The peculiar chemical characteristics of hot corino sources and WCCC sources have extensively been studied so far. However, their intermediate case, i.e. the hybrid chemistry, is suggested to be the standard case (Oya et al. 2017).

The above picture is regarded as the competition between the time scales for the chemical equilibrium and the adsorption of molecules after the UV shielding (Higuchi et al. 2018; Oya 2022); the former is roughly estimated to be $\sim 3 \times 10^5$ yr for a wide range of the H_2 density, while the latter is inversely proportional to the H_2 density. The balance of these time scales is expected to suffer from environmental effects. For instance, a strong UV radiation resets the chemical composition, and then carbon atoms are expected to tend to be adsorbed onto dust grains before they are converted to CO molecules. In a cloud supported by strong turbulence, the chemical equilibrium is expected to be achieved in the gas phase during the relatively slow cloud collapse. This qualitative understanding is actually consistent with the observational study for the 36 Class 0/I protostellar sources in the Perseus by Higuchi et al. (2018).

3. Chemistry Associated with Physical Structures

In practice, the chemical differentiation described in Section 2.1 is much more entangled with the actual physical structures. An interesting case was reported for IRAS 16293–2422 in Ophiuchus ($d \sim 140$ pc Ortiz-León et al. 2017). IRAS 16293–2422 is a Class 0 low-mass protostellar binary source, consisting of Source A and Source B. Both of them are famous as hot corinos rich in COMs (e.g. van Dishoeck et al. 1995; Cazaux et al. 2003). Especially, Source B has extensively been studied in the chemical survey project (Jørgensen et al. 2016).

Studies for kinematic structures have been performed for Source A. Source A is reported to be a multiple source, consisting at least two protostars A1 and A2 (e.g. Chandler et al. 2005; Maureira et al. 2020). The rotating gas in Source A has been reported (e.g. Pineda et al. 2012; Favre et al. 2014). Oya & Yamamoto (2020) reported that the rotating structure is resolved into the circummultiple structure of Source A and the circumstellar disk of the protostar A1. They found that the chemical composition of the gas is different between these two physical structures. Figure 4 shows the position-velocity diagrams of molecular lines tracing the rotating motion in Source A. The $C^{17}O$ and OCS emission trace the circummultiple structure extending over 300 au, while the H_2CS emission traces the circumstellar disk around the protostar A1. The kinematic structures of the circummultiple structure and the circumstellar disk can be approximated by an infalling-rotating motion and the Keplerian motion, respectively. The emission of CH_3OH and $HCOOCH_3$, which are characteristic to the famous hot corino activity of this source, were found to be locally enhanced in a ring-like structure with a radius of 50 au (Oya et al. 2016). It is interesting that this radius corresponds to the boundary between the circummultiple structure and the circumstellar disk.

A possible interpretation of the localized emission of COMs is their sublimation from dust grains by a local increase of the gas and dust temperature. The rotation temperature of H_2CS was evaluated to be highest (> 300 K) near the periastron of the circummultiple structure, and to be less than or comparable to 100 K inside and outside it (Oya et al. 2016; Oya & Yamamoto 2020), although this feature was not confirmed by Maureira et al. (2020). This situation can be caused, for instance, by a weak accretion shock by the infalling gas and by radiation heating on a possible piled-up gas. If the dust temperature locally increases at the periastron of the circummultiple structure, it would help

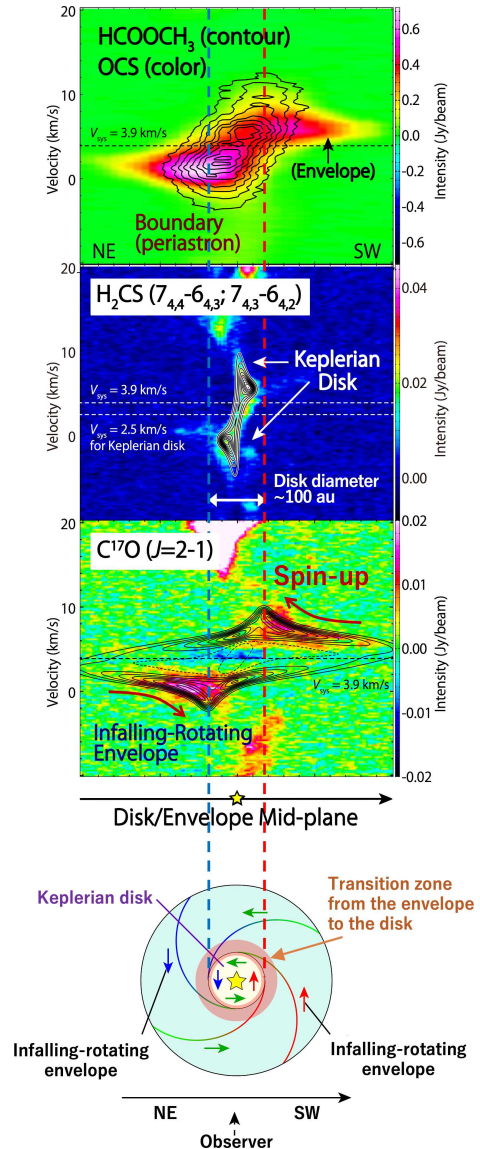


Figure 4. Transition from the infalling-rotating envelope to the Keplerian disk observed in IRAS 16293–2422 Source A. Upper panels show the position-velocity diagrams of four molecular lines, where the position axis is taken along the mid-plane of the disk/envelope system. Bottom panel shows the schematic illustration of the disk/envelope system; the circummultiple structure surrounds Source A while the circumstellar disk is associated to the protostar A1 in Source A, although the multiplicity is omitted in this panel. The chemical composition of the gas drastically changes across the boundary between the envelope and the disk. Panels for the observational data are taken from Oya et al. (2016) and Oya & Yamamoto (2020) with modifications.

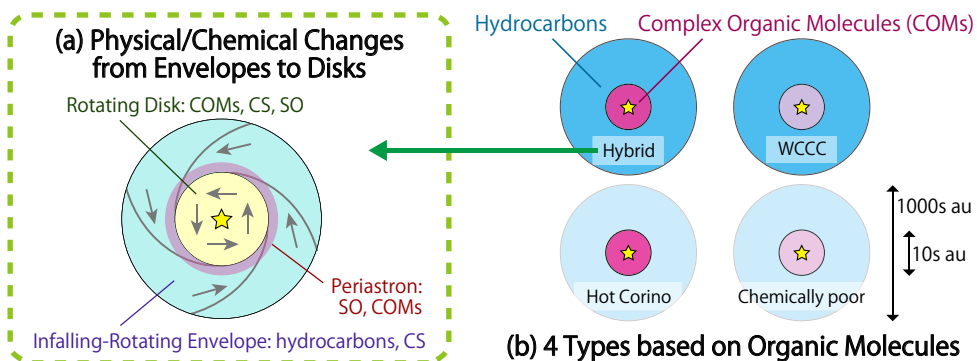


Figure 5. (a) Schematic illustration of the relation between the physical structures and the chemical composition of the gas in a disk-forming region of a young low-mass protostellar source. See Section 3 for the detail. (b) Schematic illustration of the chemical differentiation and its diversity based on organic molecules in the gas-phase. See Sections 2.1 and 2.2 for the detail.

COMs to sublimate from dust grains there. That is, the chemical change is found to be attributed to the physical structure and the gas dynamics. This may be related to the origin of the famous hot corino activity in IRAS 16293–2422 Source A. Similar chemical differentiation was confirmed in IRAS 16293–2422 Source B (Oya et al. 2018), which was utilized to examine the kinematic structure in its almost face-on disk/envelope system.

4. Overall View of Organic Molecules

Our current understandings described in the previous sections can be summarized as Figure 5. The study of the organic molecules in young low-mass protostellar sources had a large progress in this decade; the chemical diversity in protostellar cores found with single-dish telescopes can be spatially resolved by ALMA (Figure 5b). WCCC occurs at a 10^3 au scale, while hot corino chemistry occurs at a smaller scale in the vicinity of the protostar. The recent high spatial-resolution observations revealed that some sources show both the two chemical characteristics; the hybrid chemistry is likely the most standard case. Another extreme case is also found with neither the two kinds of characteristics even at a spatial resolution of 10s au (Oya et al. 2019). This is the overall trend from 10^{3-4} au scale down to a 10^{1-2} au scale.

It should be noted that the picture shown in Figure 5(b) is merely a rough classification. The actual chemical composition need to be further examined not only by the presence/absence of the organic molecules in the gas phase but, of course, by to what amount of them exist in the gas- and ice-phase. Some specific study cases show that how extent the chemical characteristics can affect the apparent chemical composition. L483, which is identified to be a hybrid chemistry source with ALMA (Figure 1), rather looks to be a carbon-chain rich source with the 45-m radio telescope at Nobeyama Radio Observatory (Hirota et al. 2009); the COM emissions on a 10s au scale is severely diluted with the beam size of 10^4 au with the single-dish telescope. COM emissions have not firmly been detected toward IRAS 15398–3359 other than CH_3OH (Jørgensen et al. 2013; Oya et al. 2014; Okoda et al. 2021) even with the high spatial-resolution and sensitivity of ALMA observations. Nevertheless, Yang et al. (2022) revealed that various COMs are indeed produced in this source and trapped in the icy grain mantle based on their observation with Mid-Infrared Instrument (MIRI) on James Webb Space Telescope (JWST).

The chemical differentiation from an infalling-rotating envelope to a Keplerian disk found in IRAS 16293–2422 (Section 3) has also been reported for other sources (Oya et al. 2022, and literatures therein). Moreover, the molecular species showing the chemical differentiation is different among sources depending on their chemical characteristics. The case for the hybrid

source L483 is shown in Figure 5(a). That is, the chemical diversity known in the parent cores is indeed delivered into the scale of the disk formation. The chemical change and its diversity can affect the material inheritance from the interstellar gas to protostellar disks, and possibly planets.

The ALMA large project FAUST (Fifty AU Study of the chemistry in the disk/envelope system of Solar-like protostars) is now being progressed to establish this unified picture of the physical/chemical view with more number of target sources and molecular species. As discussed so far, it should be emphasized that the molecular line emissions are deeply related to the physical condition *in the past* and *at present*.

5. Transition Zone from Envelopes to Disks

In these years, the chemical view and the physical structures in protoplanetary disks, including their substructures, have extensively been examined, for instance in the ALMA large projects MAPS (Molecules with ALMA at Planet-forming Scales; Öberg et al. 2021) and DSHARP (Disk Substructures at High Angular Resolution Project; Andrews et al. 2018). Meanwhile, our current understandings for younger evolutionary stages (Figure 5) would be a too simplified picture. In reality, the situation can be much more complicated at a smaller scale. One of the current problem is what is occurring in the transition zone from accreting gas to rotationally-supported disks.

5.1. Variation among Molecular Species

In IRAS 16293–2422 Source A (Section 3), the chemical composition of the gas is different between the circumstellar disk of the protostar A1 and the vicinity of the protostar A2. Its multiplicity may affect the chemical evolution from the accreting gas to protostellar disks. (The figure with preliminary results are dropped from this book.)

Not only for multiple systems, a variety of radial chemical distributions have recently been recognized as a common occurrence. For instance, ring-like distributions in protoplanetary disks were revealed in the ALMA large project ALMA-DOT (ALMA chemical survey of Disk-Outflow sources in Taurus; Garufi et al. 2021); some molecular species are thought to be destructed by molecules sublimated in the vicinity of the protostar and/or UV radiation. On the contrary, some molecular emissions are enhanced only near the protostar; observational works for Nitrogen-bearing organic molecules have extensively been reported in these years (Nazari et al. 2021). Their distributions tend to be compact relative to the Oxygen-bearing organic molecules (Okoda et al. 2021). We need a higher-angular resolution to characterize the chemical change within disks structures. Moreover, asymmetric or localized distributions are also found near protostars. Gas dynamics is an important factor; as well as the accretion shocks at the periastron (Section 3), streamers are now in the spot light (e.g. Harsono et al. 2023).

5.2. Variation within One Species

There is another complexity; the chemical composition does not always correspond to the physical structure one by one in the actual observational studies. OCS is one example, as shown in Figure 6. The OCS emission traces the outflow structure in NGC 2264 (Shibayama et al. 2021). Meanwhile, the OCS emission does not trace the outflow lobes in L1157, but is detected only in the shocked regions (Benedettini et al. 2007). In the L1551 and IRAS 16293–2422 Source A, the OCS emissions are mainly detected in their disk/envelope systems rather than the outflows (Takakuwa et al. 2020; Oya et al. 2021). SO is another example; the SO emission is known to be enhanced in shocked regions (e.g. L1157 B1 Bachiller & Pérez Gutiérrez 1997), including the accretion shocks at the periastron. The SO emission traces

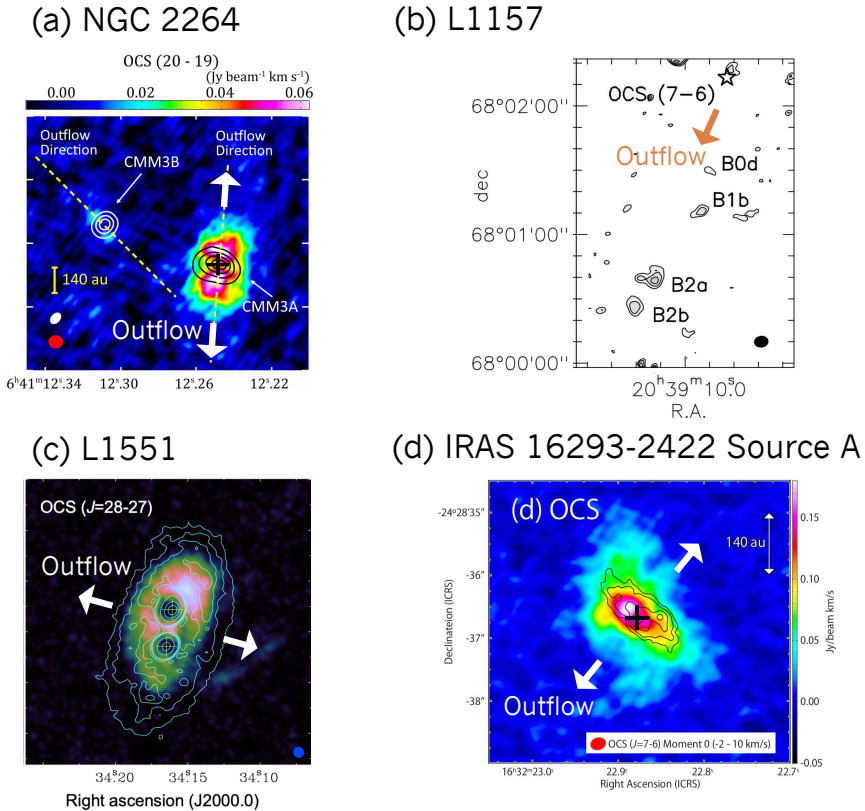


Figure 6. Observations of the OCS emission in four different sources. (a) The OCS ($J = 20 - 19$) emission is detected in the outflow of a Class 0 intermediate source NGC 2264 CMM3A. Taken from [Shibayama et al. \(2021\)](#). (b) The OCS ($J = 7 - 6$) emission is detected in the shocked regions by the outflow in L1157. Taken from [Benedettini et al. \(2007\)](#). (c) The OCS ($J = 28 - 27$) emission traces the circumbinary disk in L1551 IRS5. Taken from [Takakuwa et al. \(2020\)](#). (d) The OCS ($J = 7 - 6$) emission traces the circummultiple structure of a Class 0 protostellar source IRAS 16293–2422 Source A and is weakly detected in the outflow. Taken from [Oya et al. \(2021\)](#).

the overall morphology of the outflow in IRAS 16293–2422 Source A ([Oya et al. 2021](#)). Meanwhile, it has recently been reported that the SO emissions can trace the disk/envelope systems (B335, L483, IRAS 15398–3359; [Imai et al. 2016](#); [Oya et al. 2017](#); [Okoda et al. 2018](#)).

It is well known that some specific molecules can work as tracers; for instance, SiO is thought to be a shock tracer, and categorization of some other species are suggested by [Tychoniec et al. \(2021\)](#) as well as shown in Figure 5(a). However, some species can trace various structures depending on the characteristics of sources. We need careful consideration which molecular species trace which structure *in each source*. Sulfur-bearing species are tend to show this feature in disk-forming regions of protostellar sources, as described above. With this in mind, we are now conducting a survey with ALMA to reveal their distributions in young low-mass protostellar sources.

6. Prospects for Next Decades

The new questions discussed in the previous sections will be hot topics in the next decade.

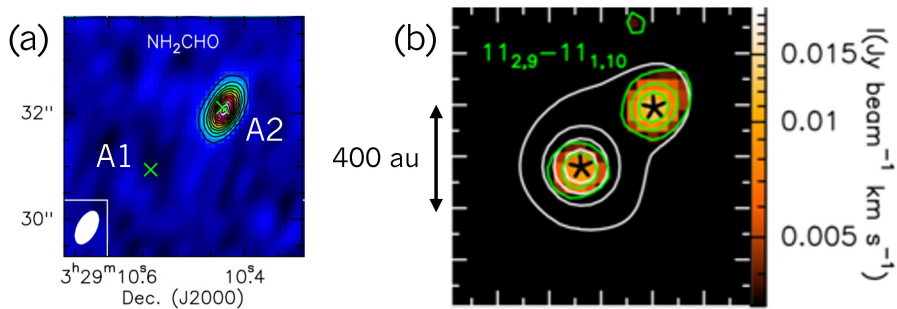


Figure 7. Emission of COMs in IRAS 4A. (a) The NH_2CHO ($12_{0,12} - 11_{0,11}$) emission is detected only in the vicinity of the protostar IRAS 4A2 with ALMA. Taken from López-Sepulcre et al. (2017) with modifications. (b) The CH_3OH ($11_{2,9} - 11_{1,10}$) emission is detected in the vicinity of both the two protostars with VLA. Taken from De Simone et al. (2020).

6.1. How to Look into the Scale for the Planetary Formation?

As extensively discussed in this symposium, one important key to solve the complexity in the vicinity of the protostars is the ice chemistry (see also Section 4). As well, the observations at the cm-wavelength will be essential. Development and enhancement of telescopes are expected to open a new avenue for this field; such as ALMA 2, Square Kilometer Array (SKA), and next generation Very Large Array (ngVLA). We can achieve a spatial resolution even as high as a few au, however, the gas in such a closest vicinity of protostars is often opaque at mm/sub-mm wavelength. The case in IRAS 4A1 is shown as an example in Figure 7. The observation of the NH_2CHO emission seems as if the two protostars would have different chemical characteristics (Figure 7a). However, non-detection of this COM emission was explained by the attenuation due to the optically thick dust continuum emission at mm/sub-mm wavelength (De Simone et al. 2020); in fact, multiple lines of CH_3OH were indeed detected at cm-wavelength with VLA (Figure 7b).

Moreover, the chemical complexity will be further examined at cm-wavelength, because there are line emissions of larger and heavier molecular species in comparison to mm/sub-mm wavelength. We are expecting to directly look into the scale of the planetary formation with a wide variety of organic molecules.

6.2. How to Cook the Huge Pile of Observational Data?

Complex physical and chemical structures have recently been found in young low-mass protostellar sources, as described in the previous sections. To solve the problems in these complexities, one direction is to make full use of the huge amount of data. We have flood of observational data in these days; for instance, archival systems of observatories and the public data of large projects. Figure 8 shows an example of numerous molecular lines detected at once with ALMA. We need to consider how to cook such a huge pile of data efficiently.

As discussed in the previous sections, the studies of chemical compositions and the physical structures are inseparable. Then, a comprehensive examination in the three-dimensional cube data for each of these various molecular emissions are required to fully use the information obtained in observations. Figure 9 shows the actual situation we have. In the position-velocity diagrams with a wide range of frequency (Figure 9c), we see similar tilted structures for many times along the mid-plane of the disk/envelope system (Figure 9a). Each of them corresponds to one molecular emission. Each molecular line traces the velocity gradient due to the gas motion, as seen in the C^{17}O emission shown in Figure 9(b) as an example. We have many

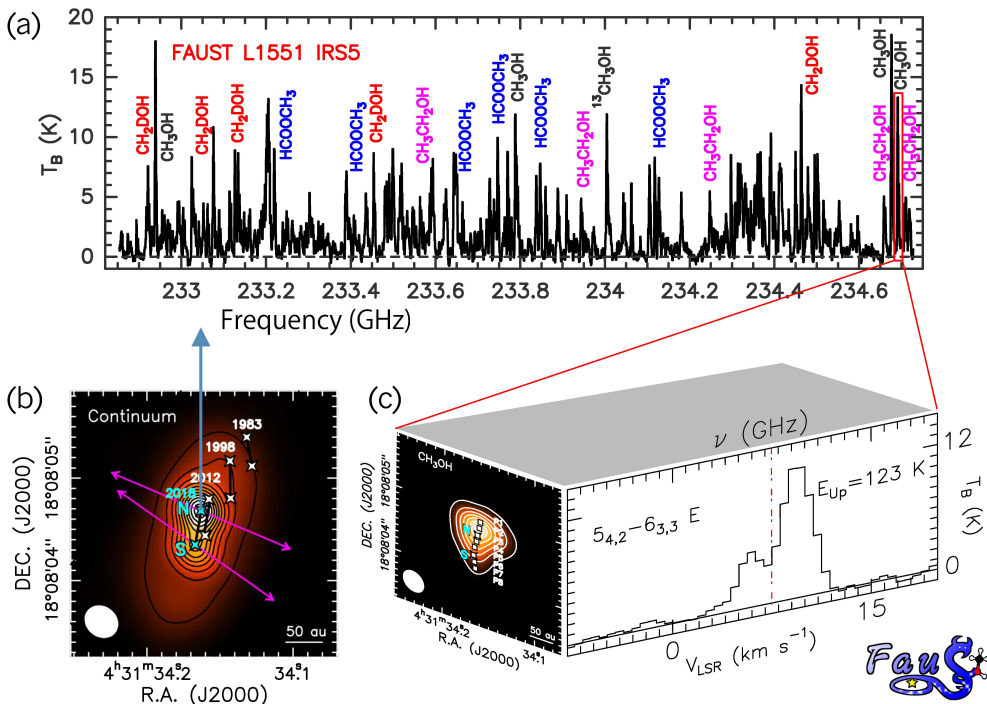


Figure 8. Observation for L1551 IRS5 as a part of the ALMA large project FAUST. Panels are taken from [Bianchi et al. \(2020\)](#) and modified. (a) Spectra taken toward the continuum peak IRS5 N. (b) Map of the 1.3 mm dust continuum emission. (c) Integrated intensity map of the CH_3OH ($5_{4,2} - 6_{3,3}$; E) emission and its spectral profile toward the continuum peak IRS5 N.

molecular emissions, and simultaneously, the information of their kinematic structures. It is, unfortunately, too hard to examine all this flood of information one by one manually.

One possible solution to resolve this tough situation is applying machine and deep learnings. [Oya et al. \(2022\)](#) performed a supervised machine learning method; the observed cube-data of the molecular lines are classified into the infalling-rotating envelope and the Keplerian disk with the aid of the support vector machine. They demonstrated that the analysis in the kinematics can help us to interpret the observed chemical view.

Conversely, the chemical diagnostics can be a powerful tool to analyze the gas dynamics. For instance, [Oya et al. \(2021\)](#) examined the re-distribution of the angular momentum of the gas during the disk formation among the accreting gas, the rotating disk, and the outflow. Rotating motion of outflows have been detected in several sources in these years (e.g. [Hirota et al. 2017](#); [Oya et al. 2018](#); [Zhang et al. 2018](#)). Because a possible rotation motion of an outflow is expected to be most prominent near its launching point with the smallest radial size ([Oya et al. 2015](#)), it is essential to find a suitable molecular tracer to avoid a contamination from the disk/envelope component there. This approach is not limited for low-mass protostellar sources. There would be a chance to apply to other rotating structures, such as high-mass sources ([Olguin et al. 2023](#)) and even active galactic nuclei ([Aalto et al. 2020](#)). These rotating structures have much different spatial scales, but can have some analogies in physics. This may provide us with a clue to the structure formation with angular momentum.

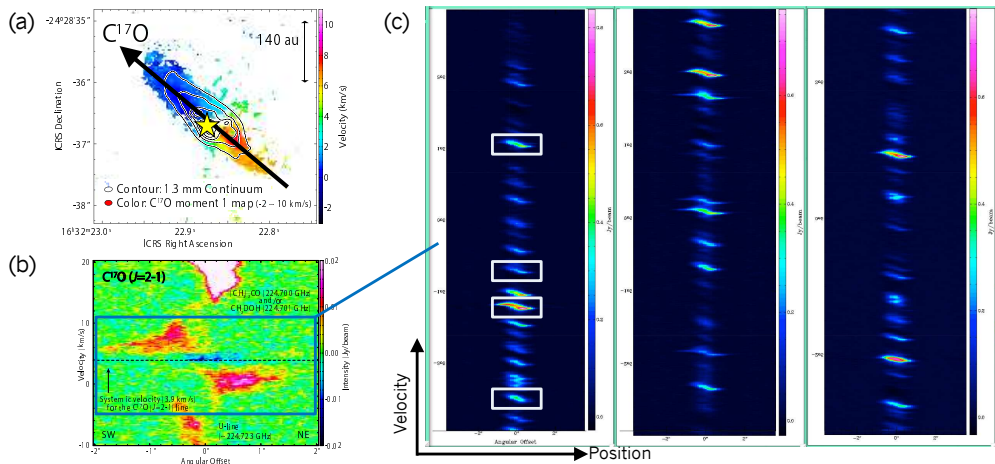


Figure 9. Kinematic structure in IRAS 16293–2422 Source A. Panels (a) and (b) are taken from Oya & Yamamoto (2020) and modified. (a) Velocity map (moment 1 map) of the $C^{17}O$ emission. The velocity gradient is seen along the northeast-southwest direction due to the infall and rotation motion surrounding the multiple system. (b) Position-velocity diagram of the $C^{17}O$ emission. The position axis is taken along the mid-plane of the circummultiple structure, as represented by the arrow in panel (a). (c) Position-velocity diagram of three spectral windows prepared along the disk/envelope system. The observational data is taken from the PILS (The ALMA Protostellar Interferometric Line Survey) survey with ALMA (Jørgensen et al. 2013).

7. Summary

As discussed so far, we have some progresses to fill out the missing-link in the disk-formation study in these years. We see *the co-evolution of the chemical compositions and the physical structures*. As the molecular distributions are classified by comparing with simple physical models, the study in the chemical composition is inseparable from the information in the kinematics.

The next step is looking into the planet-forming regions. As for the structure formation process, re-distribution of the angular momentum has an essential role to determine the initial condition for the planet formation. The chemical evolution along this gas dynamics will be an important clue to the material origin of planets. Meanwhile, the study in planetary systems are going to have extensive progresses, for example with Hayabusa-2 and JWST. We are still on the way to bridge our understandings from the star-formation study to the planetary science.

References

- Aalto, S., Falstad, N., Muller, S., et al. 2020, *A&A*, 640, A104. doi:10.1051/0004-6361/202038282
- Aikawa, Y., Wakelam, V., Garrod, R. T., et al. 2008, *ApJ*, 674, 984. doi:10.1086/524096
- Andrews, S. M., Huang, J., Pérez, L. M., et al. 2018, *ApJL*, 869, L41. doi:10.3847/2041-8213/aaf741
- Bachiller, R. & Pérez Gutiérrez, M. 1997, *ApJL*, 487, L93. doi:10.1086/310877
- Benedettini, M., Viti, S., Codella, C., et al. 2007, *MNRAS*, 381, 1127. doi:10.1111/j.1365-2966.2007.12300.x
- Bianchi, E., Chandler, C. J., Ceccarelli, C., et al. 2020, *MNRAS*, 498, L87. doi:10.1093/mnras/ltaa130
- Cazaux, S., Tielens, A. G. G. M., Ceccarelli, C., et al. 2003, *ApJL*, 593, L51. doi:10.1086/378038
- Ceccarelli, C. 2004, *Star Formation in the Interstellar Medium: In Honor of David Hollenbach*, 323, 195
- Chandler, C. J., Brogan, C. L., Shirley, Y. L., et al. 2005, *ApJ*, 632, 371. doi:10.1086/432828
- De Simone, M., Codella, C., Ceccarelli, C., et al. 2020, *A&A*, 640, A75. doi:10.1051/0004-6361/201937004

- Favre, C., Jørgensen, J. K., Field, D., et al. 2014, *ApJ*, 790, 55. doi:10.1088/0004-637X/790/1/55
- Fuller, G. A., Lada, E. A., Masson, C. R., et al. 1995, *ApJ*, 453, 754. doi:10.1086/176437
- Lefloch, B., Bachiller, R., Ceccarelli, C., et al. 2018, *MNRAS*, 477, 4792. doi:10.1093/mnras/sty937
- Maureira, M. J., Pineda, J. E., Segura-Cox, D. M., et al. 2020, *ApJ*, 897, 59. doi:10.3847/1538-4357/ab960b
- Garufi, A., Podio, L., Codella, C., et al. 2021, *A&A*, 645, A145. doi:10.1051/0004-6361/202039483
- Harsono, D., Bjerkele, P., Ramsey, J. P., et al. 2023, *ApJL*, 951, L32. doi:10.3847/2041-8213/acdfca
- Higuchi, A. E., Sakai, N., Watanabe, Y., et al. 2018, *ApJS*, 236, 52. doi:10.3847/1538-4365/aabfe9
- Hirota, T., Ohishi, M., & Yamamoto, S. 2009, *ApJ*, 699, 585. doi:10.1088/0004-637X/699/1/585
- Hirota, T., Machida, M. N., Matsushita, Y., et al. 2017, *Nature Astronomy*, 1, 0146. doi:10.1038/s41550-017-0146
- Imai, M., Sakai, N., Oya, Y., et al. 2016, *ApJL*, 830, L37. doi:10.3847/2041-8205/830/2/L37
- Imai, M., Oya, Y., Sakai, N., et al. 2019, *ApJL*, 873, L21. doi:10.3847/2041-8213/ab0c20
- Imai, M., Oya, Y., Svoboda, B., et al. 2022, *ApJ*, 934, 70. doi:10.3847/1538-4357/ac77e7
- Jørgensen, J. K., Visser, R., Sakai, N., et al. 2013, *ApJL*, 779, L22. doi:10.1088/2041-8205/779/2/L22
- Jørgensen, J. K., van der Wiel, M. H. D., Coutens, A., et al. 2016, *A&A*, 595, A117. doi:10.1051/0004-6361/201628648
- Öberg, K. I., Guzmán, V. V., Walsh, C., et al. 2021, *ApJS*, 257, 1. doi:10.3847/1538-4365/ac1432
- Okoda, Y., Oya, Y., Sakai, N., et al. 2018, *ApJL*, 864, L25. doi:10.3847/2041-8213/aaad8ba
- Okoda, Y., Oya, Y., Francis, L., et al. 2021, *ApJ*, 910, 11. doi:10.3847/1538-4357/abddb1
- Olguin, F. A., Sanhueza, P., Chen, H.-R. V., et al. 2023, *ApJL*, 959, L31. doi:10.3847/2041-8213/ad1100
- Ortiz-León, G. N., Loinard, L., Kounkel, M. A., et al. 2017, *ApJ*, 834, 141. doi:10.3847/1538-4357/834/2/141
- Oya, Y., Sakai, N., Sakai, T., et al. 2014, *ApJ*, 795, 152. doi:10.1088/0004-637X/795/2/152
- Oya, Y., Sakai, N., Lefloch, B., et al. 2015, *ApJ*, 812, 59. doi:10.1088/0004-637X/812/1/59
- Oya, Y., Sakai, N., López-Sepulcre, A., et al. 2016, *ApJ*, 824, 88. doi:10.3847/0004-637X/824/2/88
- Oya, Y., Sakai, N., Watanabe, Y., et al. 2017, *ApJ*, 837, 174. doi:10.3847/1538-4357/aa6300
- Oya, Y., Moriwaki, K., Onishi, S., et al. 2018, *ApJ*, 854, 96. doi:10.3847/1538-4357/aaa6c7
- Oya, Y., Sakai, N., Watanabe, Y., et al. 2018, *ApJ*, 863, 72. doi:10.3847/1538-4357/aacf42
- Oya, Y., López-Sepulcre, A., Sakai, N., et al. 2019, *ApJ*, 881, 112. doi:10.3847/1538-4357/ab2b97
- Oya, Y. & Yamamoto, S. 2020, *ApJ*, 904, 185. doi:10.3847/1538-4357/abbe14
- Oya, Y., Watanabe, Y., López-Sepulcre, A., et al. 2021, *ApJ*, 921, 12. doi:10.3847/1538-4357/ac0a72
- Oya, Y., Kibukawa, H., Miyake, S., et al. 2022, *PASP*, 134, 094301. doi:10.1088/1538-3873/ac8839
- Oya, Yoko. “A Few Tens au Scale Physical and Chemical Structures Around Young Low-Mass Protostars.”, 2022, *Springer Nature*. doi:10.1007/978-981-19-1708-0
- López-Sepulcre, A., Sakai, N., Neri, R., et al. 2017, *A&A*, 606, A121. doi:10.1051/0004-6361/201630334
- Nazari, P., van Gelder, M. L., van Dishoeck, E. F., et al. 2021, *A&A*, 650, A150. doi:10.1051/0004-6361/202039996
- Pineda, J. E., Maury, A. J., Fuller, G. A., et al. 2012, *A&A*, 544, L7. doi:10.1051/0004-6361/201219589
- Rice, E. L., Prato, L., & McLean, I. S. 2006, *ApJ*, 647, 432. doi:10.1086/505326
- Sakai, N. & Yamamoto, S. 2013, *Chemical Reviews*, 113, 8981. doi:10.1021/cr4001308
- Schöier, F. L., Jørgensen, J. K., van Dishoeck, E. F., et al. 2002, *A&A*, 390, 1001. doi:10.1051/0004-6361:20020756
- Shibayama, Y., Watanabe, Y., Oya, Y., et al. 2021, *ApJ*, 918, 32. doi:10.3847/1538-4357/ac0ef6
- Takakuwa, S., Saigo, K., Matsumoto, T., et al. 2020, *ApJ*, 898, 10. doi:10.3847/1538-4357/ab9b7c
- Tychoniec, Ł., van Dishoeck, E. F., van't Hoff, M. L. R., et al. 2021, *A&A*, 655, A65. doi:10.1051/0004-6361/202140692
- Yang, Y.-L., Green, J. D., Pontoppidan, K. M., et al. 2022, *ApJL*, 941, L13. doi:10.3847/2041-8213/aca289
- van Dishoeck, E. F., Blake, G. A., Jansen, D. J., et al. 1995, *ApJ*, 447, 760. doi:10.1086/175915
- van Gelder, M. L., Tabone, B., Tychoniec, Ł., et al. 2020, *A&A*, 639, A87. doi:10.1051/0004-6361/202037758
- Zhang, Y., Higuchi, A. E., Sakai, N., et al. 2018, *ApJ*, 864, 76. doi:10.3847/1538-4357/aad7ba